9-2011

Quantifying Forest Aboveground Carbon Pools And Fluxes Using Multi-Temporal Lidar

Lee Spangler
Montana State University, spangler@montana.edu

Lee A. Vierling
University of Idaho, leev@uidaho.edu

QUANTIFYING FOREST ABOVEGROUND CARBON POOLS AND FLUXES USING MULTI-TEMPORAL LIDAR

A report on field monitoring, remote sensing MMV, GIS integration, and modeling results for forestry field validation test to quantify aboveground tree biomass and carbon

September 2011

U.S. Department of Energy (DOE)
National Energy Technology Laboratory (NETL)
DOE Award Number: DE-FC26-05NT42587

Submitted by: Dr. Lee Spangler

BSCSP Principal Investigator and Director
Montana State University
P.O. Box 173905
Bozeman, MT 59717
spangler@montana.edu
http://www.bigskyco2.org
Phone: (406) 994-4399
Fax: (406) 994-3745

BSCSP Forestry Team

Lee A. Vierling (correspondent: leev@uidaho.edu)
Eva K. Stand
Andrew T. Hudak
Jan U.H. Eitel
Sebastian Martinuzzi

Disclaimer

Table of Contents

Figures

Tables

Abstract

Sound policy recommendations relating to the role of forest management in mitigating atmospheric carbon dioxide (CO_2) depend upon establishing accurate methodologies for quantifying forest carbon pools for large tracts of land that can be dynamically updated over time. Light Detection and Ranging (LiDAR) remote sensing is a promising technology for achieving accurate estimates of aboveground biomass and thereby carbon pools; however, not much is known about the accuracy of estimating biomass change and carbon flux from repeat LiDAR acquisitions containing different data sampling characteristics.

In this study, discrete return airborne LiDAR data was collected in 2003 and 2009 across ~20,000 hectares (ha) of an actively managed, mixed conifer forest landscape in northern Idaho, USA. Forest inventory plots, established via a random stratified sampling design, were established and sampled in 2003 and 2009. The Random Forest machine learning algorithm was used to establish statistical relationships between inventory data and forest structural metrics derived from the LiDAR acquisitions. Aboveground biomass maps were created for the study area based on statistical relationships developed at the plot level.

Over this 6-year period, we found that the mean increase in biomass due to forest growth across the non-harvested portions of the study area was 4.8 metric ton/hectare (Mg/ha). In these non-harvested areas, we found a significant difference in biomass increase among forest successional stages, with a higher biomass increase in mature and old forest compared to stand initiation and young forest. Approximately 20% of the landscape had been disturbed by harvest activities during the six-year time period, representing a biomass loss of >70 Mg/ha in these areas. During the study period, these harvest activities outweighed growth at the landscape scale, resulting in an overall loss in aboveground carbon at this site. The 30-fold increase in sampling density between the 2003 and 2009 did not affect the biomass estimates.

Overall, LiDAR data coupled with field reference data offer a powerful method for calculating pools and changes in aboveground carbon in forested systems. The results of our study suggest that multitemporal LiDAR-based approaches are likely to be useful for high quality estimates of aboveground carbon change in conifer forest systems.

1. Introduction

Forests cover approximately one third of the Earth's land surface. They have a tremendous potential to store and cycle carbon (Harmon and Marks, 2002), and therefore represent a crucial component of the global carbon cycle. The Food and Agriculture Organization of the United Nation's Global Forest Resources Assessment (FRA, 2005) estimates that the world's forests store 283 Gigatonnes (Gt) of carbon in their biomass alone, and that the total carbon stored in forested ecosystems, including live and dead wood, litter, detritus, and soil, exceeds the amount of carbon found in the atmosphere. Because of continued pressure on forest resources to provide environmental services for the ever growing global human population, the interest in quantifying carbon pools and fluxes over large geographic areas has increased over the past decades. In particular, forest carbon-related research includes:

- quantifying the role of forest dynamics in the global carbon cycle,
- assessing human impacts (e.g. harvest, prescribed fire, land use change) on forest carbon flux and storage,
- estimating how natural forest processes (i.e. insect attacks, wildfires, windthrow) affect the global carbon cycle,
- providing carbon accounting to satisfy local- to global-scale policy agreements,
- quantification of timber volume and growth for commercial interests, and
- assessment of carbon storage in the context of maintaining biodiversity and wildlife habitat quality and connectivity.

Regardless of the reason for inquiry, and process by which forest carbon storage changes, it is critical to establish repeatable, objective, and accurate methods for estimating aboveground forest carbon pools and fluxes over large areas. Direct, diurnal-scale measurements of the carbon exchange between forests and the atmosphere are commonly accomplished with measurements from continental- and global-scale networks of eddy covariance flux towers (e.g. Schwalm et al. 2007). These methods are extremely valuable in quantifying net carbon exchange between the biosphere and the atmosphere; however, the estimates can be noisy, affected by windy conditions and structurally complex vegetation and topography, and limited in geographic extent (Hollinger and Richardson 2005). Ecosystem process models, such as Biome-BGC, Forest-BGC, 3PG and 3PG-S, are useful for better understanding of carbon pools and fluxes in forests (Running and Coughlan 1988, Running and Gower 1991, Landsberg and Waring 1997, Coops et al. 1998, Waring et al. 2010).

Integration of these ecosystem process models with remote sensing of land surface characteristics have greatly improved our ability to make regional assessments of carbon pools and fluxes (e.g. Turner et al. 2004). Although information from passive remote sensing (e.g. Advanced Very High Resolution Radiometer [AVHRR], Moderate Resolution Imaging Spectroradiometer [MODIS], Landsat) have contributed to regional estimates of Gross Primary Production (GPP) and Net Primary Production (NPP), challenges remain in optimizing the spatial resolution of remotely sensed data for specific applications and differentiating the relative influences of vegetation structure and chemical variables (Turner et al. 2004). As a result, efforts to quantify forest growth (i.e. change in aboveground carbon pools) using traditional passive remote sensing imagery have had limited success (Yu et al. 2008).

Remote sensing approaches for quantifying forest structure and volume are rapidly evolving. Vine and Sathaye (1997) suggest that in order to quantify aboveground forest carbon pools and fluxes across broad extents, it is important to combine remote sensing techniques with carbon estimation methods that are based on existing standard forest inventory principles. Light Detection and Ranging (LiDAR) has been successfully employed for characterizing vertical structure and forest attributes such as canopy height distribution, tree height, and crown diameter (Nilsson 1996, Hudak et al. 2002, Lefsky et al. 2002, Yu et al. 2008). However, although processes governing forest biomass pools are highly dynamic in time, almost all LiDAR-based studies aimed at quantifying carbon pools have been based upon single-date data acquisitions, and are therefore limited to providing estimates at a single point in time. Robust methods for producing wall-to-wall maps of above ground forest carbon using LiDAR combined with field data collections and Monte Carlo methods have recently been developed with errors < 1% (Gonzales et al. 2010).

Time series remote sensing studies have been used to estimate both carbon pools and net change in aboveground carbon. In a study by Asner et al. (2003), researchers studied pools and fluxes of carbon in semiarid woodlands, using texture analysis of black and white aerial photographs from 1937 compared to spectral mixture analysis of Landsat data from 1999 to estimate the change in above ground woody carbon pools and the net flux over the 62 year time period. Strand et al. (2008) estimated net change in above ground woody carbon over a 52 year time period using 2-D spatial wavelet analysis on time series black and white aerial photography and allometric relationships. Tree growth in a conifer plantation was estimated over a 19 year time period using synthetic aperture radar (SAR) backscattering changes, with a resulting root mean square error (RMSE) in tree growth of 8.2 meters (m) (Balzter et al. 2003). Yu et al. (2008) used multi-temporal LiDAR acquisitions (10 points/m^2) to predict volume and mean height growth in mixed multi-story boreal forests in Finland with a standard deviation of the residuals of 0.15-0.30 m for mean height growth. While these studies showed promise for multi-temporal LiDAR based assessment of forest growth, additional work remains to extend this approach to the quantification of carbon (biomass) in forests over time.

The objective of this research is therefore to combine multi-temporal LiDAR remote sensing with forest inventory surveys and statistical modeling to characterize carbon pools and predict rates of aboveground carbon sequestration in managed mixed conifer forests of the Northern Rocky Mountains (USA). This project builds on forest inventory data collection and a LiDAR acquisition from the summer of 2003 (Evans and Hudak 2007), complemented with similar data acquisitions from 2009. We quantify the impact on forest growth and timber harvest on forest carbon pools across the landscape, and examine relationships among changes in these pools during this 6-year interval with respect to forest height and successional status. We anticipate that our work will not only serve to quantify forest carbon fluxes and pools, but will also establish additional rationale for acquiring LiDAR data of forest land across the United States.

2. Methods

2.1 *Study Area*

The study is centered in the Palouse Range (~20,000 hectares [ha]; Latitude 46° 48′ N, Longitude 116° 52′ W), located in northern Idaho, USA (Figure 1). The area is topographically complex, ranging from 780 m to 1520 m in elevation. Climate is characterized by a warm dry summer and fall, and a wet winter and spring when most of the mean annual average precipitation of 630 – 1015 millimeters (mm) falls in the form of snow in the winter and rain in the spring. Vegetation is primarily comprised of temperate mixed-conifer forest with dominant species being Ponderosa pine (*Pinus ponderosa* C. Lawson var. scopulorum Engelm.), Douglas-fir (*Pseudotsuga menziesii* (Mirb.) Franco var. glauca (Beissn.) Franco), grand fir (*Abies grandis* (Douglas ex D. Don) Lindl.), western red cedar (*Thuja plicata* Donn ex D. Don), and western larch (*Larix occidentalis* Nutt).

The land ownership is dominated by private timber companies with many private and public land inholdings. Inholdings include a large tract of University of Idaho experimental forest land, the watershed for the city of Troy, Idaho, and a small parcel of old-growth western red cedar managed by Latah county and protected for biodiversity conservation. The variety of habitat types and the unique management goals and strategies of each of the landowners, has created a forest that is diverse in species composition, stand age, and structure, representing a variety of biophysical settings and forest successional stages (Falkowski et al. 2009). Major disturbances occurring during the time period 2003 to 2009 include forest management such as harvest, thinning, and prescription fire. The study area is bounded to the north, west, and south by highly productive dryland agricultural fields producing crops that include wheat, lentils, and chick peas.

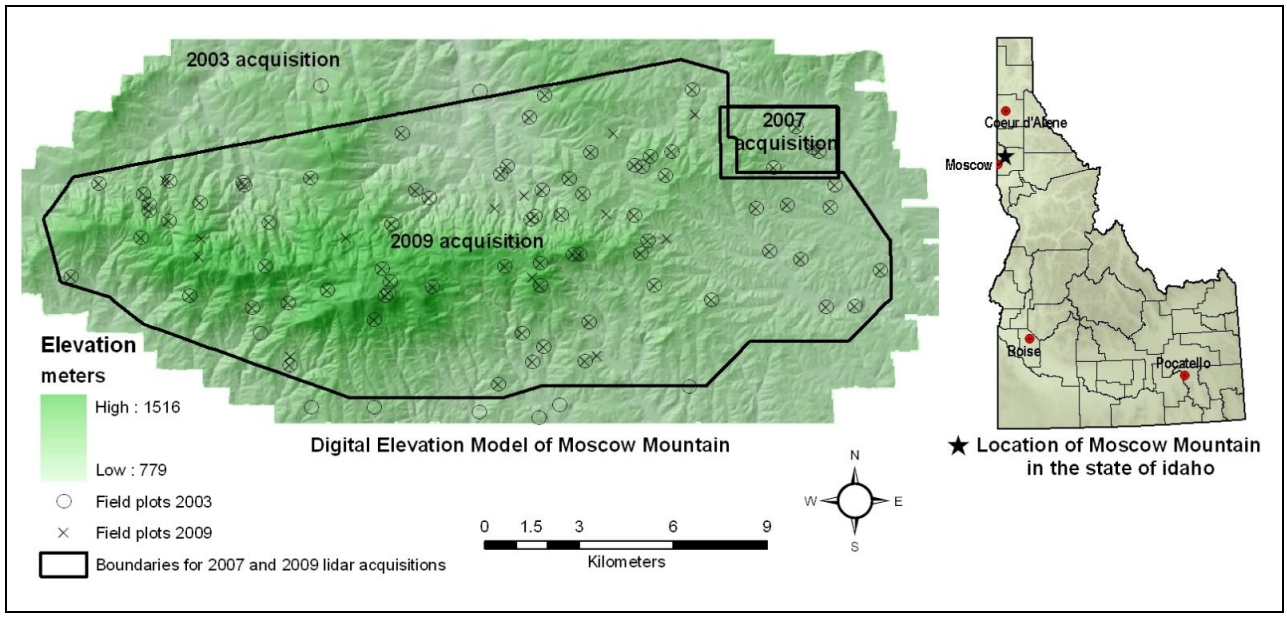

Figure 1: Location of the Moscow Mountain study area in north central Idaho. The extent of the DEM reflects the boundary of the 2003 LiDAR survey.

2.2 *LIDAR Surveys and Processing*

LiDAR data was flown during three time periods, 2003, 2007, and 2009. The 2003 LiDAR survey was flown by Horizons, Inc. (Rapid City, SD, USA), the 2007 survey by Surdex Corporation (Chesterfield, MO, USA), and the 2009 survey by Watershed Sciences, Inc. (Portland, OR, USA). The extent of the 2003 LiDAR survey was 32,708 ha, while that of the 2007 (1,681 ha) and 2009 (19,889 ha) LiDAR surveys was a combined 20,624 ha (they overlap by 106 ha), which lies wholly within the extent of the 2003 LiDAR survey (Figure 1). Acquisition parameters of these LiDAR surveys are provided in Table 1. The difference in the LiDAR survey point densities in the acquisitions from 2003 and 2009 are illustrated in Figure 2.

Table 1: Acquisition parameters of the 2003, 2007, and 2009 LiDAR surveys

Survey Date	Altitude Above Ground	LiDAR System	Multiple Returns	Footprint Diameter	Scan Angle	Average Post Spacing	Average Point Density
Summer 2003	2438 m	ALS 40	Up to 3/pulse	30 cm	+/- 18°	1.58 m	0.40/m^2
7 July 2007	1219 m	ALS 50	Up to 4/pulse	30 cm	+/- 15°	0.41 m	5.98/m^2
30 June 2009	2000 m	ALS 50	Up to 4/pulse	30 cm	+/- 14°	0.29 m	11.95/m^2

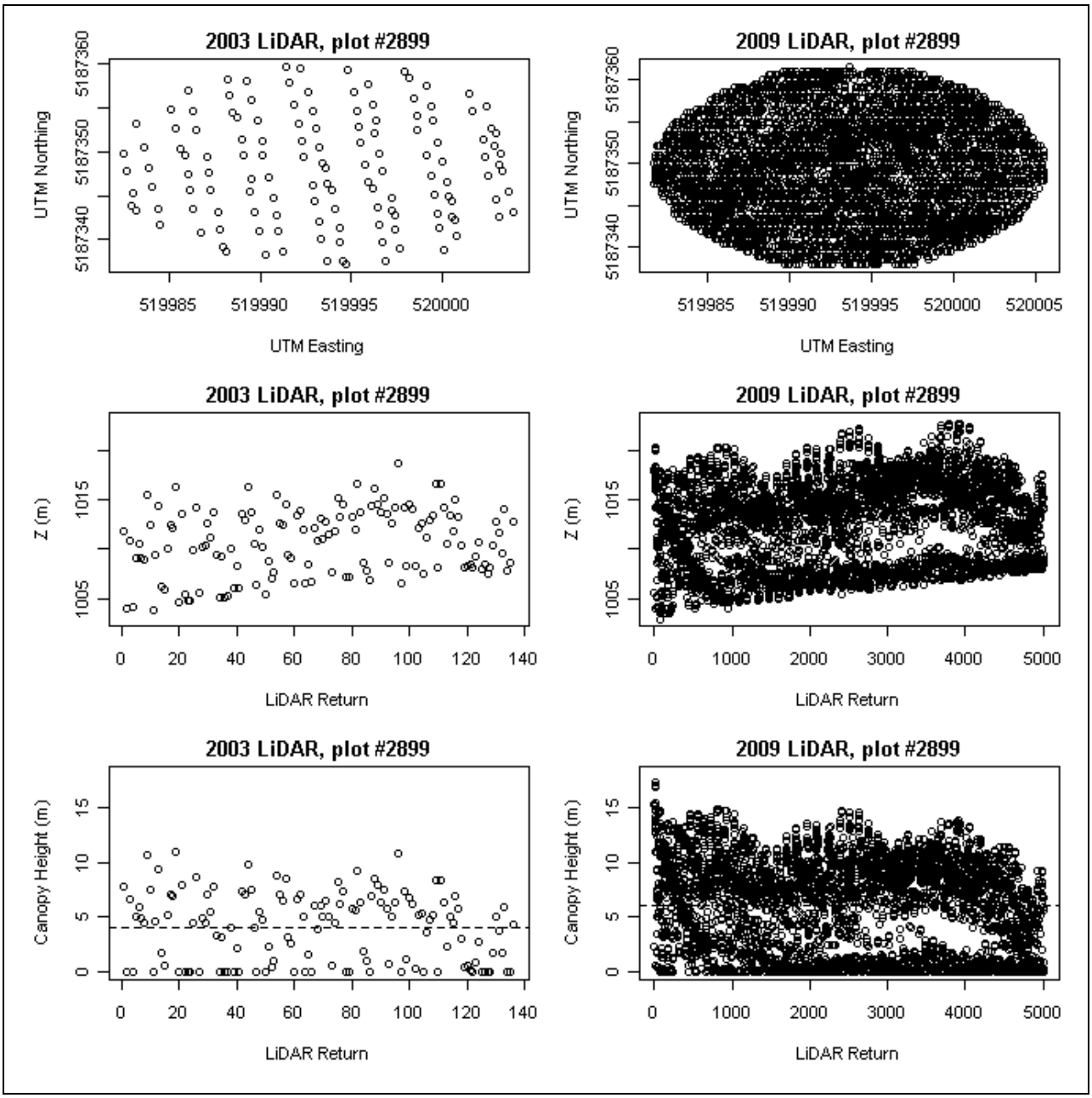

Figure 2: Comparison of LiDAR survey point densities in 2003 (0.4 points/m^2, left) and 2009 (12 points/m^2, right) at the scale of a single undisturbed 0.25-ha inventory plot (#2899), as viewed from overhead (top) and from the side before detrending for topography (middle) and after (bottom). Note that despite the 30-fold difference in point density between the two surveys, the vertical distribution of points indicative of canopy structure is consistently shaped, making the plot-level canopy height metrics directly comparable. Mean height in this plot increased 2.0 m from 2003 (4.0 m) to 2009 (6.0 m) as indicated by the dotted horizontal lines.

The 2009 LiDAR data was delivered in the common Log ASCII Standard (LAS) LiDAR format, and the libLAS library for reading and writing such data was used to extract the data into text files (http://liblas.org/). The flow of LiDAR processing steps is diagrammed in Figure 3. The data was delivered in tiles, with a size of <0.5 million points per tile. For each LiDAR point, the following characteristics were delivered:

- x and y coordinates,
- absolute elevation (z),
- the number of LiDAR returns at this location and the return number for the point, and
- the laser return intensity ranging from 0 to 255.

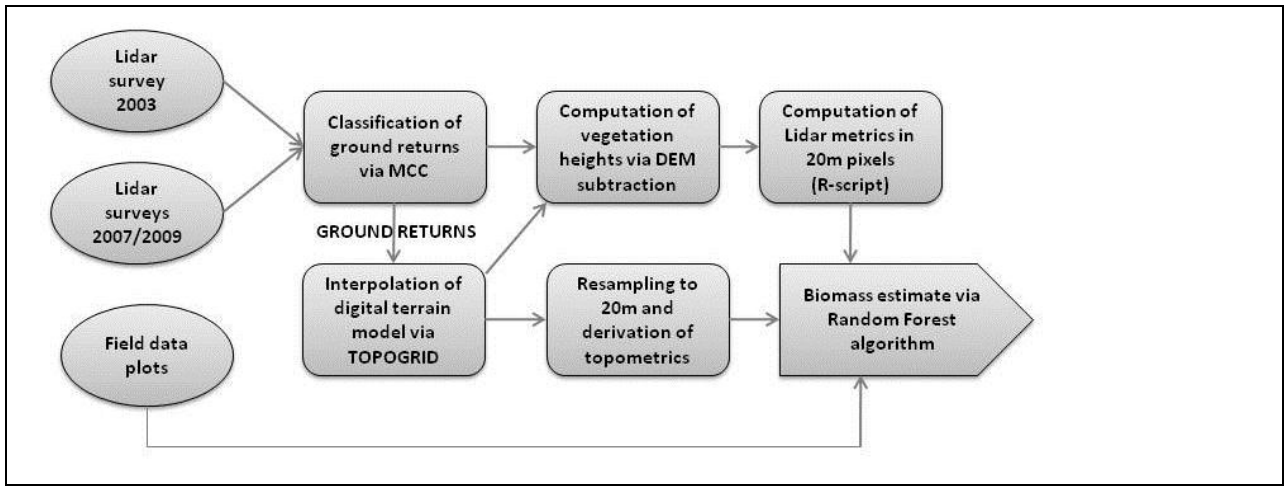

Figure 3: Procedure for deriving biomass estimates from remote sensing LiDAR data and field information. The LiDAR surveys from 2003 and 2007/2009 were processed separately to estimate above ground woody biomass followed by grid subtraction to obtain the change in biomass.

Points were converted from text format into the ArcInfo coverage format using the GENERATE command in Arc Macro Language (AML). The ground returns were separated from the vegetation returns with the multiscale curvature classification method (MCC, Evans and Hudak 2007). The scale parameter used in the MCC AML was set to match the LiDAR post-spacing, and we used a curvature parameter of 0.8, a tension parameter of 0.07 and a 5 pixel kernel. A digital terrain model of 1 m pixel resolution was created from the LiDAR ground returns through interpolation of the z values using the TOPOGRID function in ArcInfo, which generates a hydrologically correct grid of elevation from ground point data.

Because of the high density of the dataset, it was necessary to process the LiDAR data in 10 independent yet overlapping tiles that were later merged. Care was taken not to introduce edge effects in each tile by removing the overlapping edge pixels prior to merging the tiles. Vegetation height for each LiDAR return was computed by subtracting the value of the digital terrain model from the LiDAR z-value. A few instances of anomalously high points (e.g. > 100 m) representing LiDAR returns from birds or other particles in the air were removed from the

dataset. LiDAR data from the 2003 acquisition was processed in a similar fashion; see Evans and Hudak (2007) for a detailed description of the 2003 LiDAR points.

LiDAR vegetation structure metrics were computed for both the 2003 and 2009 LiDAR acquisitions based on the height and intensity of the LiDAR returns within 20 m grid cells across the study area in the statistical software package R (R Development Core Team 2007). The 1 m digital terrain model was resampled to 20 m by the bilinear resampling method in ArcInfo Grid to match the origin of the LiDAR metrics. Secondary topographic metrics were derived from the 20 m digital terrain model. LiDAR metrics were also computed within each 11.35 m radius inventory plot, and the topographic metrics were extracted from the 20 m topographic layers at each plot center.

2.3 *Field Sampling*

In 2003, the study area was stratified by elevation and solar insolation into nine unique combinations. Inventory plots were systematically placed within each stratum guided by a Landsat-derived leaf area index (Pocewicz et al. 2004). This method of stratification ensured that the forest inventory plots covered the full range of forest habitat types and canopy structure conditions across the study area. The 2003 LiDAR survey was calibrated and validated with 84 field plots, of which 76 were located within the reduced extent of the 2007 (n=4) and 2009 (n=72) LiDAR surveys. During the summer of 2003, an 11.35 m fixed-radius (404.69 m^2) forest inventory plot was installed at each sample location. The diameter at breast height (dbh), tree species, tree height, as well as distance and bearing from plot center, were measured and recorded for all trees (dbh > 2.7 cm) within the fixed radius plot. Seedlings and saplings were measured and tallied across the inventory plot. See Falkowski et al. (2005) for additional details regarding the sampling design and data collection procedures.

The 2003 field plots were given priority for populating the 2009 stratification. A new private landowner denied us permission to revisit one of our 2003 plots, so only 75 plots were re-measured. In addition, because the landscape had changed since 2003, 14 of the strata were left unfilled by existing plots, necessitating the addition of 14 new plots. This resulted in 75 + 14 = 89 plots for 2009 model calibration/validation.

2.4 *Biomass Modeling*

Models for predicting biomass were developed from the field data collected in both 2003 and 2009, using the Random Forest machine learning algorithm (Brieman 2001) based on LiDAR height metrics, intensity metrics and topographic metrics. The suite of input variables used in the Random Forest modeling is described by Hudak et al. (2008). Random Forest is a non-parametric technique that can handle both continuous and categorical independent variables. The technique uses a bootstrap approach for achieving higher accuracies compared to traditional classification tree modeling. Random Forest uses the Gini statistic for node splitting which allows for non-linear variable interactions. A large number of classification trees are produced, permutations are introduced at each node, and the most common classification result is selected. The technique has been used successfully for classifying LiDAR data into forest succession classes (Falkowski et al. 2009), for classifying passive remote sensing data into desired

vegetation classes (Falkowski et al. 2005), for characterizing mountain pine beetle infestations (Coops et al 2006) and for estimating forest structure attributes from LiDAR data (Hudak et al. 2008, Martinuzzi et al., 2009).

2.5 *Spatial Analysis*

Biomass was estimated within each 20 m pixel across the study area by applying the biomass models developed from field data via the Random Forest algorithm for the time periods 2003 and 2009. Change in biomass over the six year time period was calculated via grids in ArcInfo by subtracting the biomass estimated for 2003 from the biomass estimated for 2009.

Biomass increase within successional stages was estimated via overlay analysis between a map of successional stages developed for the same study area by Falkowski et al. (2009) and the change in biomass estimated as part of this project. Successional stages mapped by Falkowski et al. (2009) included:

- Open – treeless areas, stand initiation;
- Stand Initiation (SI) – space reoccupied by seedlings, saplings or shrubs following a stand replacing disturbance;
- Understory Reinitiation (UR) - older cohort of trees being replaced by new individuals, broken overstory with an understory stratum present;
- Young Multistory (YMS) - two or more cohorts of young trees from a variety of age classes;
- Mature Multistory (MMS) - two or more cohorts of mature trees from a variety of age classes; and
- Old Multistory (OMS) - two or more cohorts of trees from a variety of age classes, dominated by large trees.

Areas that experienced a decrease in biomass from 2003 to 2009 were excluded from the analysis to avoid impacts of human activity or natural disturbance in the successional stage growth estimates. We tested the hypothesis that there is a significant difference in biomass increase within undisturbed areas between forest successional stages with a one-way Analysis of Variance (ANOVA). Tukey's post-hoc test was employed to evaluate which of the successional stages had experienced significant differences in biomass increase over the six year period.

3. Results

3.1 *Change in Biomass*

Both the 2003 and 2009 LiDAR survey landscapes were independently stratified by elevation, insolation, and canopy cover in stratified random sampling designs. Elevation was obtained from a USGS Digital Elevation Model (DEM), and an insolation layer calculated using Solar Analyst (Fu and Rich, 1999). Canopy cover was estimated from satellite image-derived vegetation indices. Our strategy was to treat each time period as an independent assessment, as a forest manager may likely do, so both the 2003 and 2009 biomass models were developed independently based on all available contemporaneous plot measures from the 2003 (n=84) or 2009 (n=89) field surveys. Variable selection from a suite of 49 candidate LiDAR height, density, and intensity metrics was also performed separately yet consistently.

A Random Forest model selection function that uses Model Improvement Ratio (MIR) standardized importance values (Evans and Cushman 2009, Evans et al. 2010, Murphy et al. 2010) was used to choose the most important predictor variables from the suite of candidate LiDAR metrics. In the interest of parsimony, models with selected predictor variables that were highly correlated (Pearson's $r > 0.9$) were pruned to include only predictor variables with Pearson's $r < 0.9$. In cases where $r > 0.9$, the variable with lesser importance according to the MIR statistic was excluded from consideration, and the model selection function rerun to search for alternative predictors. The function selected a total of eight metrics for predicting 2003 biomass and ten metrics for predicting 2009 biomass (Table 2, Figure 4, & Figure 5). The most important metric was mean height, followed by several other height, density and intensity metrics, while no topographic metrics were selected. The Random Forest algorithm in R (R Development Team, v2.10.0) was then used to predict biomass in 2003 and 2009 from these variables (Table 2), with their importance values shown in Figure 4 and Figure 5.

Table 2: LiDAR metrics selected for the independent 2003 and 2009 biomass models.

Metric	Metric Description	2003 Biomass Model	2009 Biomass Model
hmean	Height mean	*	*
hmad	Height median absolute deviation		*
hmax	Height maximum	*	
h90th	Height 90th percentile		*
hskew	Height skewness	*	*
hiqr	Height interquartile range	*	*
crr	Canopy relief ratio	*	
stratum2	Stratum 2 canopy density		*
stratum4	Stratum 4 canopy density	*	*
stratum5	Stratum 5 canopy density	*	*
imean	Intensity mean	*	*
i10th	Intensity 10th percentile		*

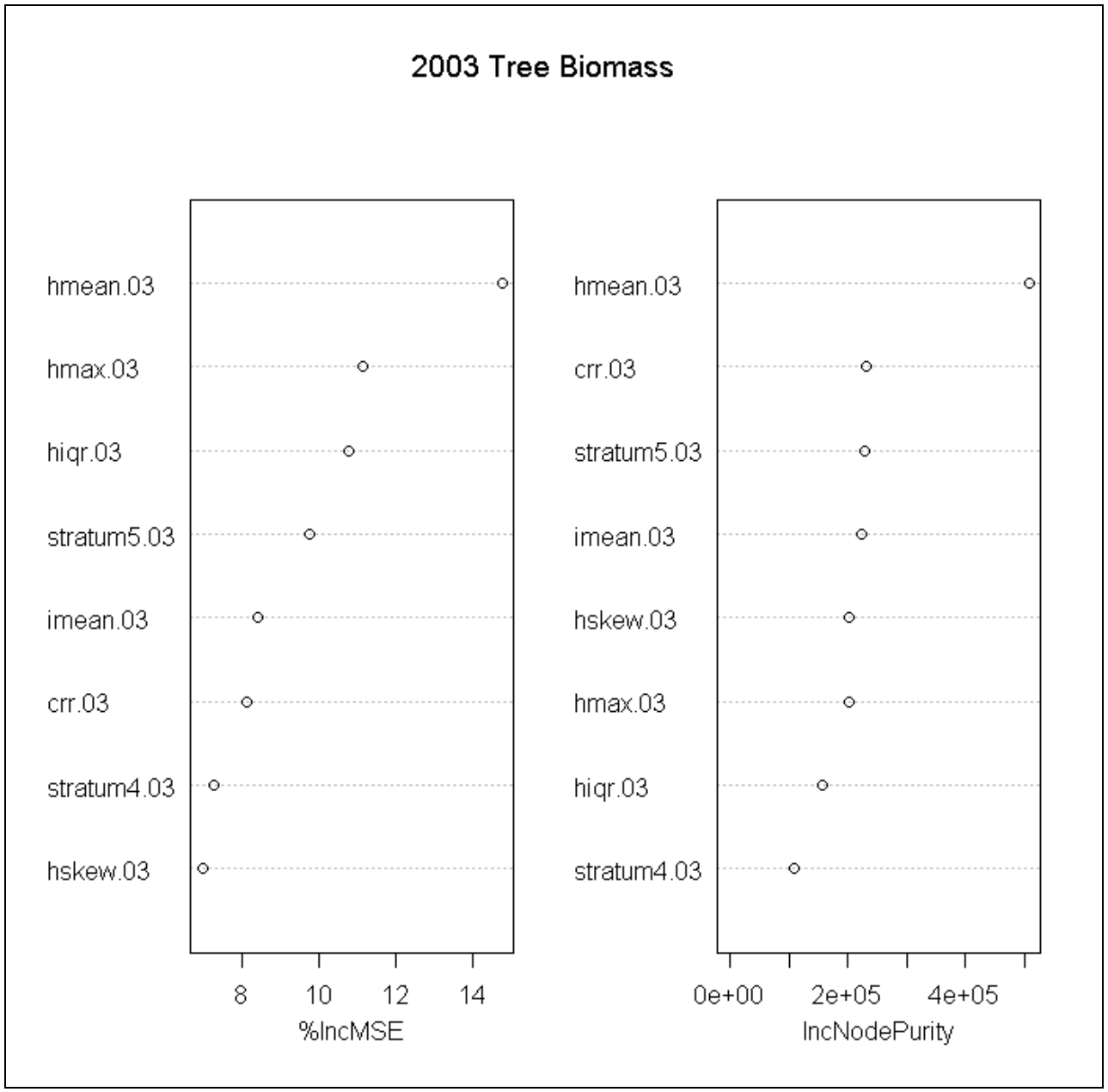

Figure 4: Random Forest variable importance measures for the 2003 biomass model according to two statistics: Mean Decrease Accuracy (%IncMSE) (left) and Mean Decrease Gini (IncNodePurity) (right). The most important variables are sorted decreasingly from top to bottom.

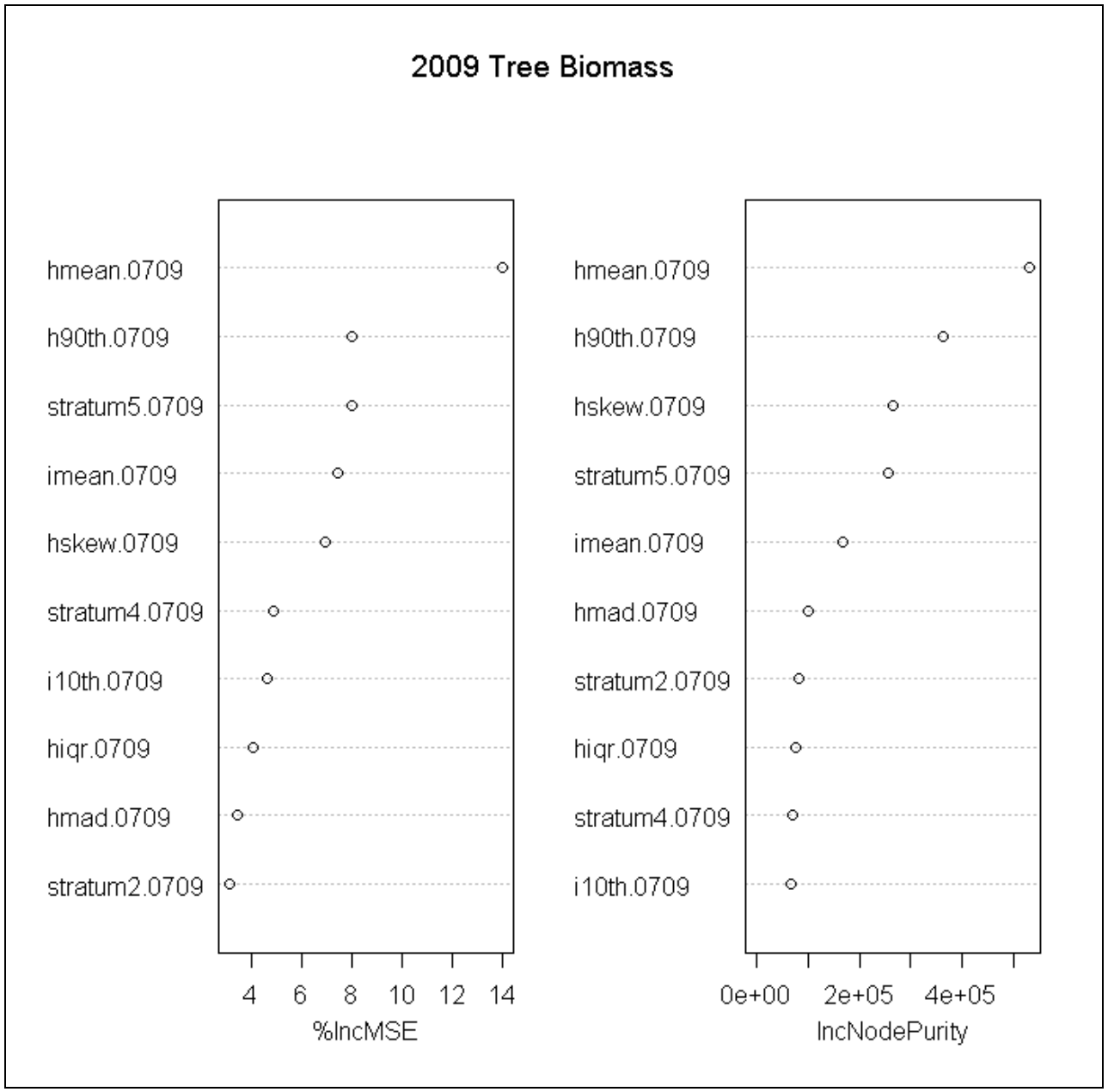

Figure 5: Random Forest variable importance measures for the 2009 biomass model according to two statistics: Mean Decrease Accuracy (%IncMSE) (left) and Mean Decrease Gini (IncNodePurity) (right). The most important variables are sorted decreasingly from top to bottom.

While the full count of plots could be used to develop the independent 2003 and 2009 biomass models, only the 75 plots common to both field surveys were available for comparing plot-level biomass predictions. Plots of predicted biomass (Figure 6) and biomass change (Figure 7) reveal considerable scatter around the 1:1 line because the models include both undisturbed and disturbed plots, as is also evident in the observations. Partitioning the data into the undisturbed and disturbed plot classes as they were called in the field reveals greater sensitivity and accuracy in the model predictions relative to observations (Figure 8). However, the difference between independent 2003 and 2009 biomass predictions was conservative, or less than observed, in both the undisturbed and disturbed plots.

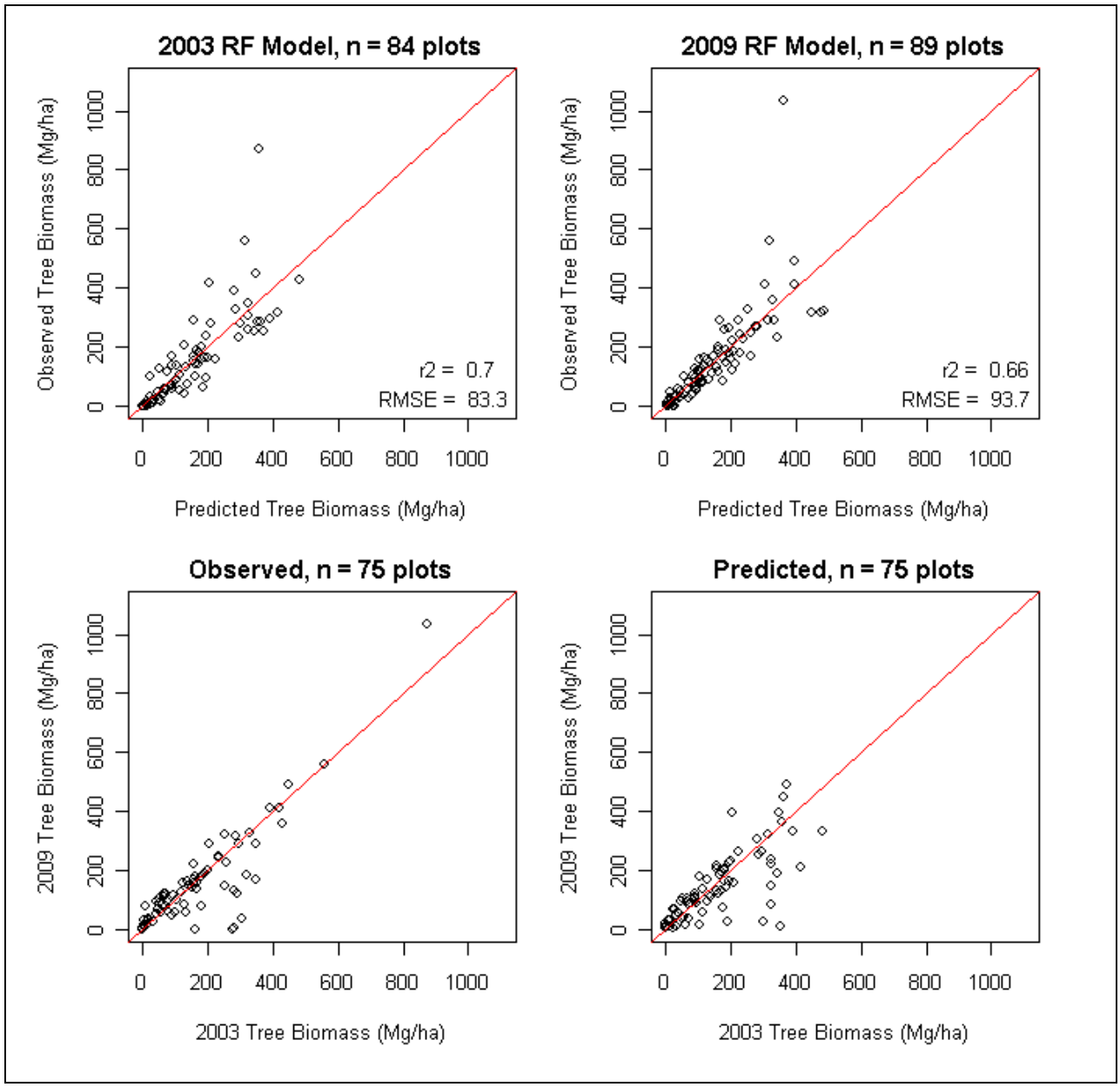

Figure 6: Predicted vs. observed aboveground tree biomass from the independent 2003 and 2009 models.

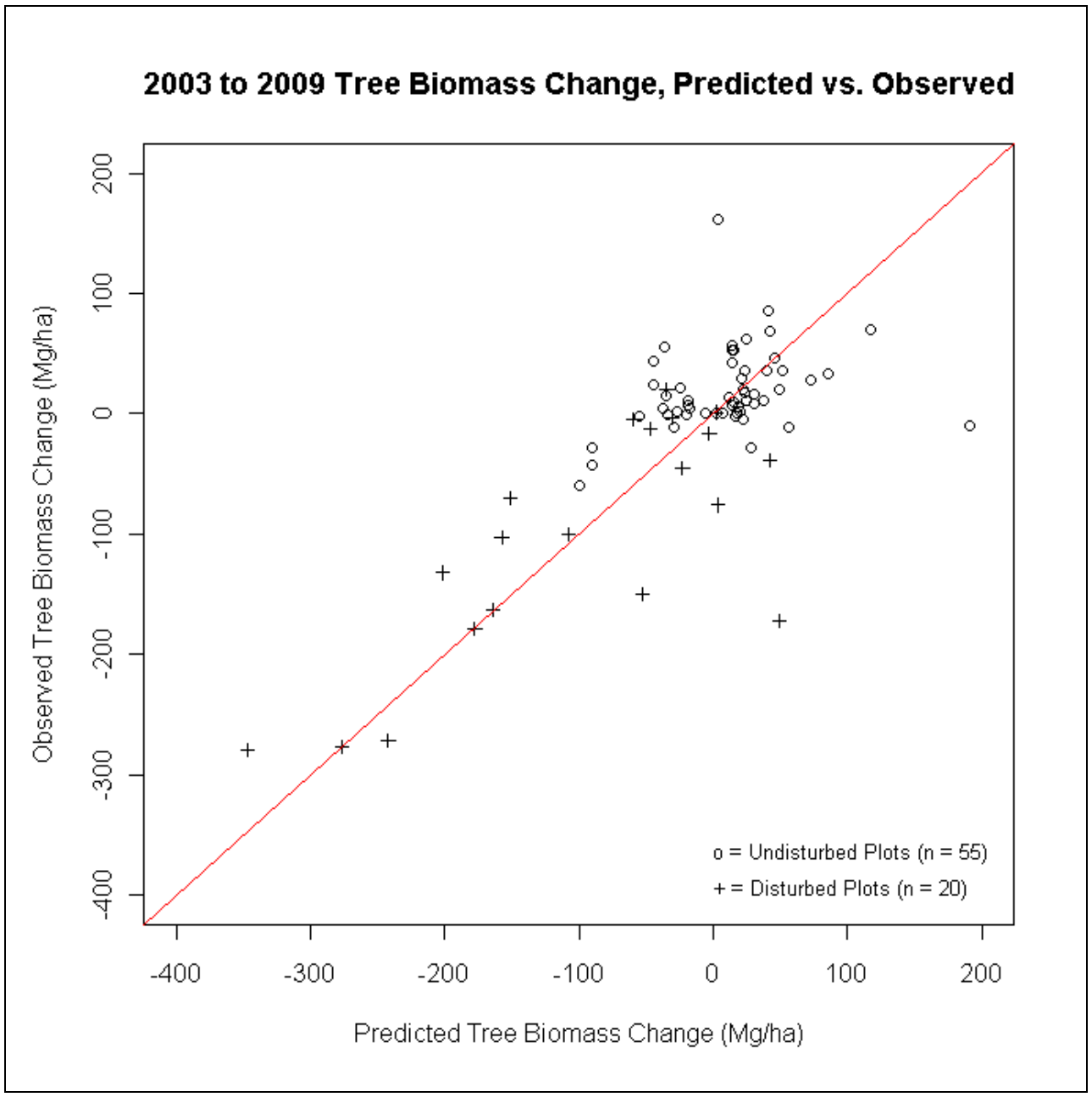

Figure 7: Predicted vs. observed aboveground tree biomass change from 2003 to 2009

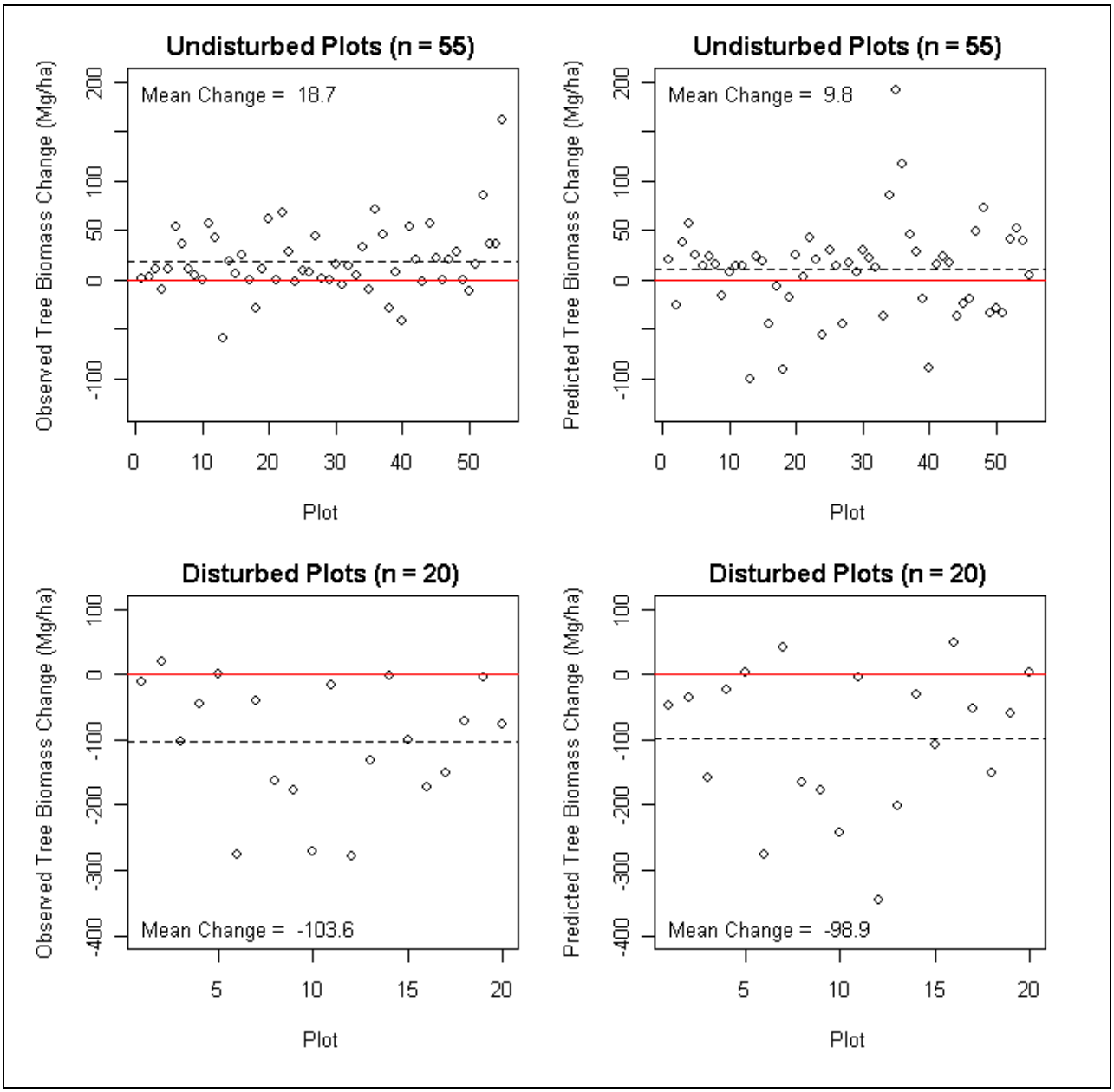

Figure 8: Observed and predicted aboveground tree biomass change in undisturbed (top) and disturbed (bottom) plots

Closer examination of the most important predictor variable in both the 2003 and 2009 models, mean canopy height, reveals the sensitivity and accuracy of the LiDAR canopy height distributions despite different point densities (Figure 9).

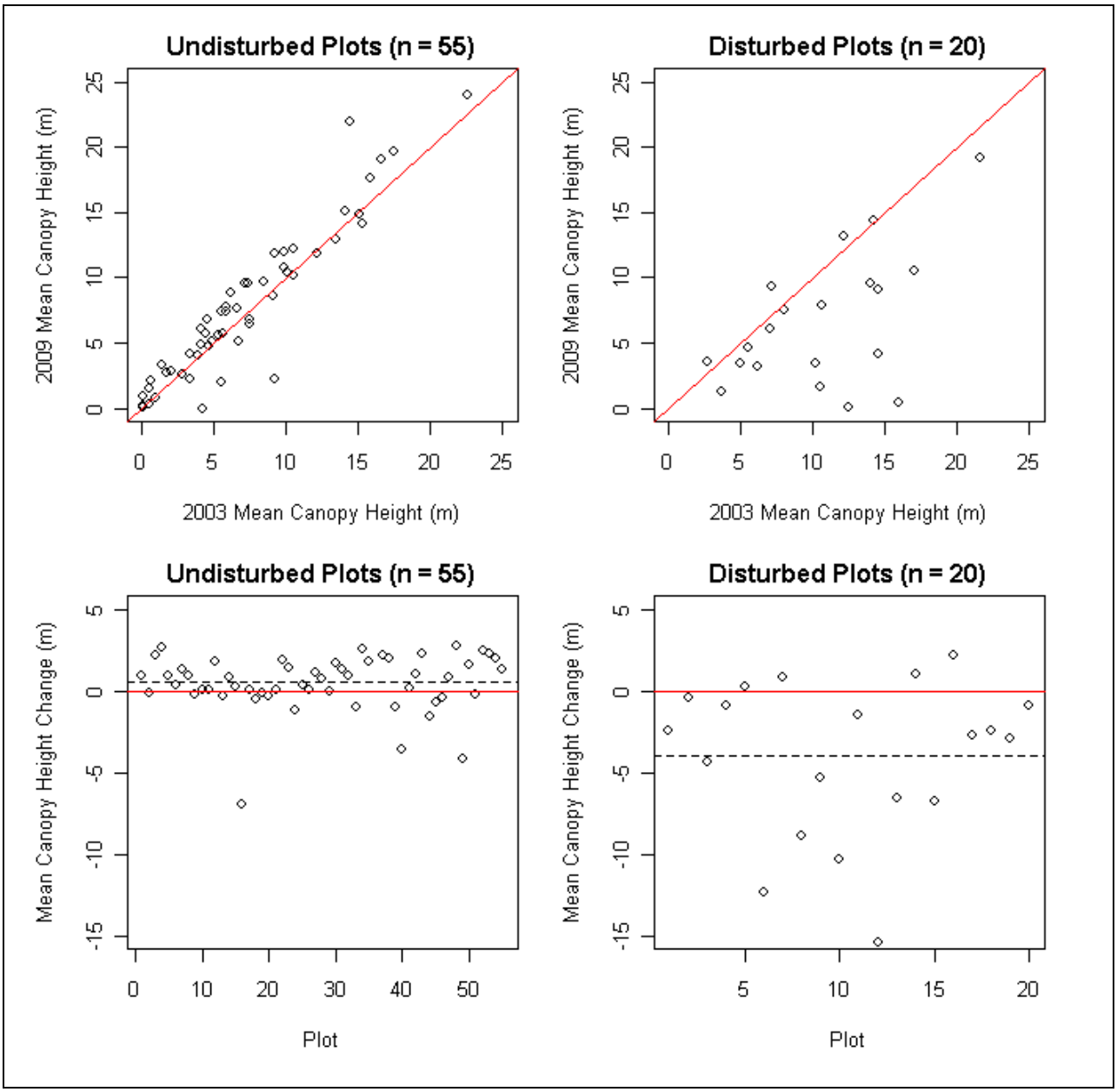

Figure 9: Mean canopy height in 2003 and 2009 and mean canopy height change in undisturbed and disturbed plots

Biomass estimates for the region were mapped at a 20 m pixel resolution based on models developed at the plot level for the two time periods 2003 and 2009 (Figure 10). Biomass change was derived by subtracting the two maps (Figure 11). Removed from consideration were nonforested agricultural areas classified from the LiDAR as having zero canopy density in both 2003 and 2009, amounting to 6.1% of the landscape, found mostly around the periphery of the study area. A histogram of the biomass change was derived for a better understanding of the biomass change distribution (Figure 12). Harvested areas in the biomass change map (Figure 11)

were defined as a loss in biomass of 70 Mg/ha or more. After six years, the mean biomass increase across the unharvested forest (73.7% of the study area), excluding nonforest agricultural areas (6.1% of study area), was 4.8Mg/ha (standard deviation 34.2 Mg/ha); mean biomass decrease in harvested forest areas (20.2% of the study area) was 185.1 Mg/ha (standard deviation 97.1 Mg/ha).

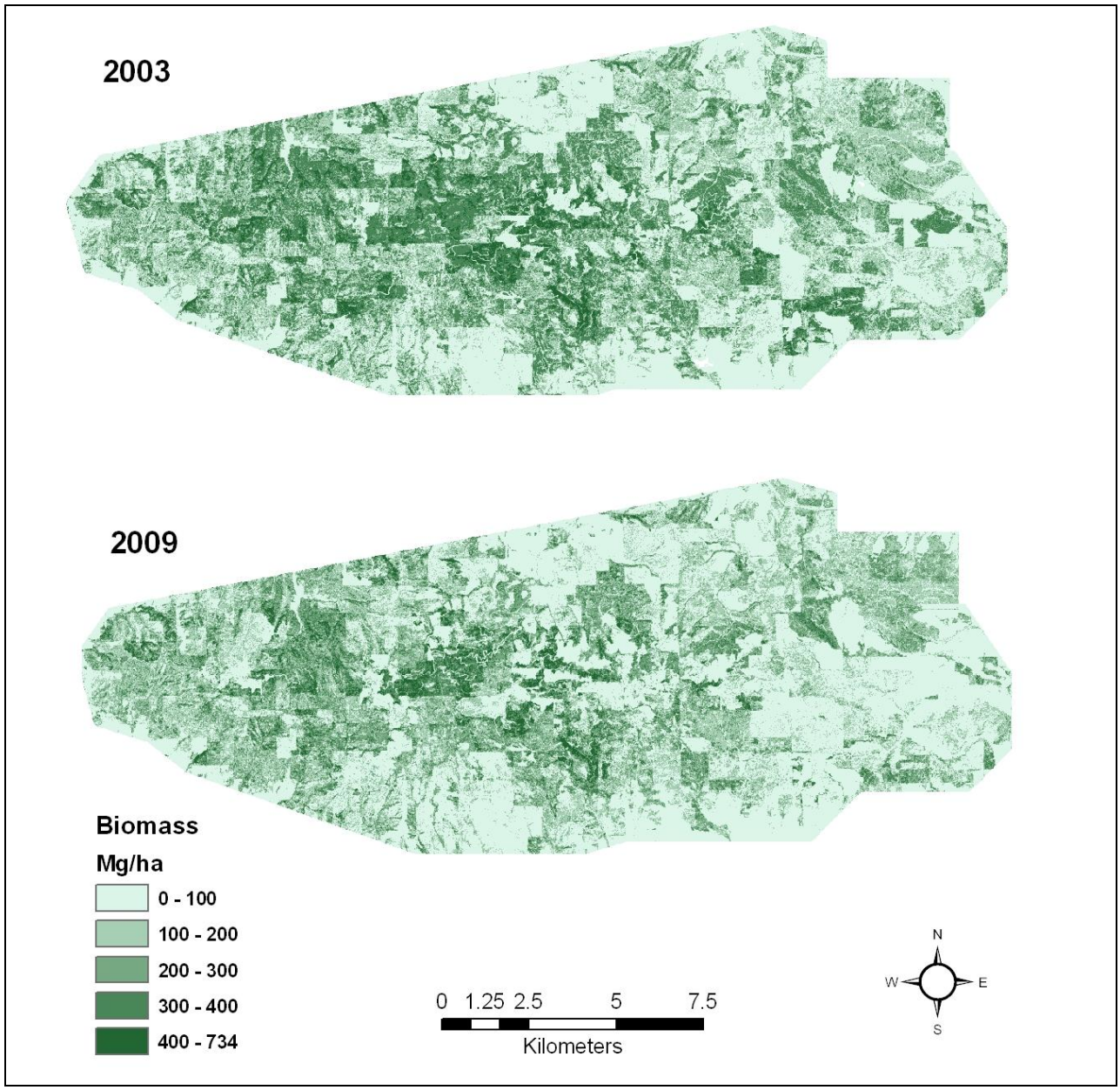

Figure 10: Mapped 2003 and 2009 aboveground tree biomass predictions across the combined extent of the 2007 and 2009 LiDAR surveys

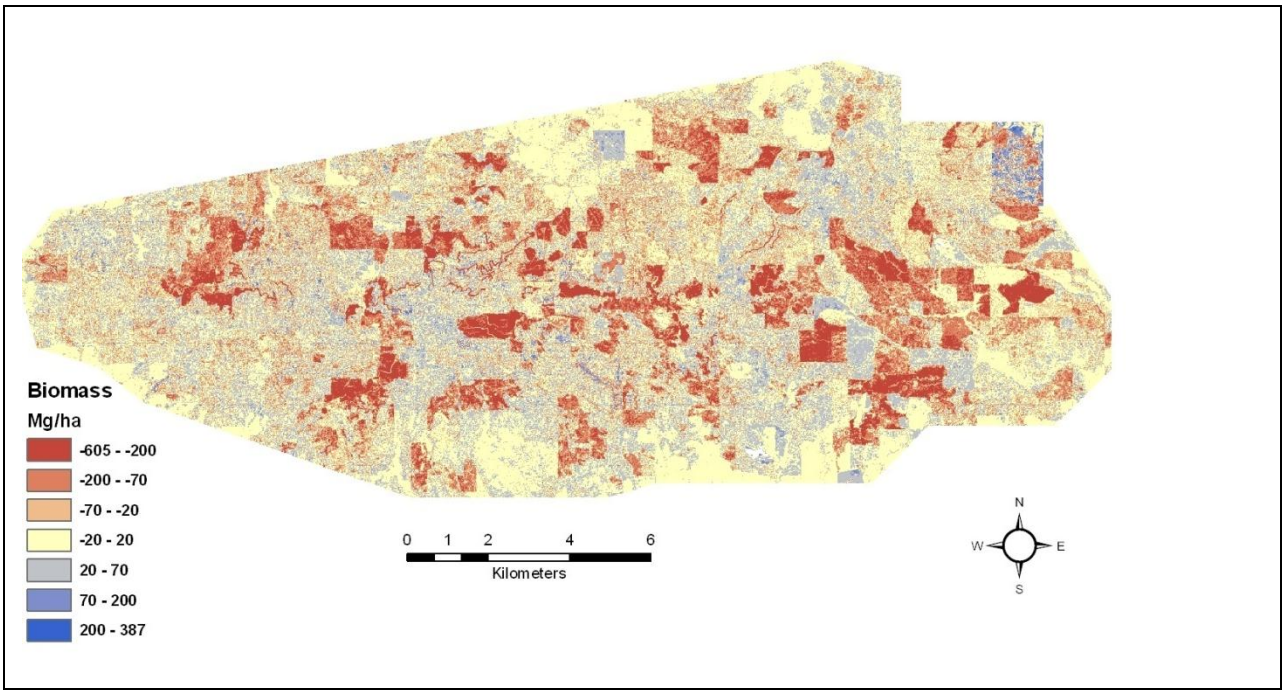

Figure 11 : Mapped 2003-2009 aboveground tree biomass change

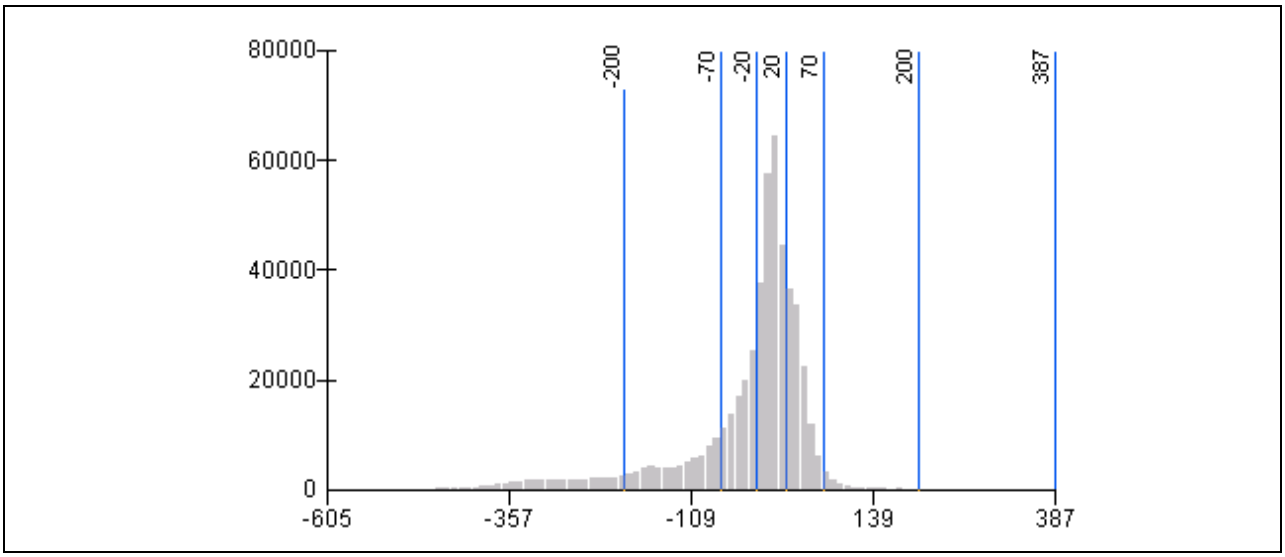

Figure 12: Histogram of biomass change with the class breaks in Fig. 11 included (y axis represents number of pixels)

Whether or not a 2003 inventory plot was disturbed was recorded during the 2009 field visits; this information was used to objectively determine a disturbance threshold. The discrepancy between biomass change observed at the field plots (Figure 8) and biomass change estimated from the maps may be attributable to field plot classifications of disturbance that included even

minor management interventions besides harvest disturbance. Of the 89 inventory plots characterized in 2009, 75 were revisited 2003 plots. Twenty of the 75 revisited plots (26.7%) were labeled as disturbed in the 2009 survey. At the landscape level, 20.2% of the 20,624 ha landscape with repeat LiDAR coverage was classified as harvested using this <= -70 Mg/ha disturbance threshold.

Predicted aboveground tree biomass and biomass change were extracted from the maps (Figure 10 & Figure 11) at the re-measured field plot locations (n=75) and at systematic 500 m intervals (n=810 samples). Plots of these data versus mean height, the most important predictor variable in both the 2003 and 2009 biomass models reveal a close linear relationship (Figure 13). The relationship of aboveground tree biomass to maximum canopy height (Figure 14) and canopy density (not shown) is curvilinear and much looser. Further examination of estimated biomass change at undisturbed sites, calculated as the difference between the 2009 and 2003 biomass predictions at the field plots and systematically sampled landscape sites, revealed no relationship between aboveground tree biomass accretion and mean canopy height; however, it did show a relationship to height growth (Figure 15).

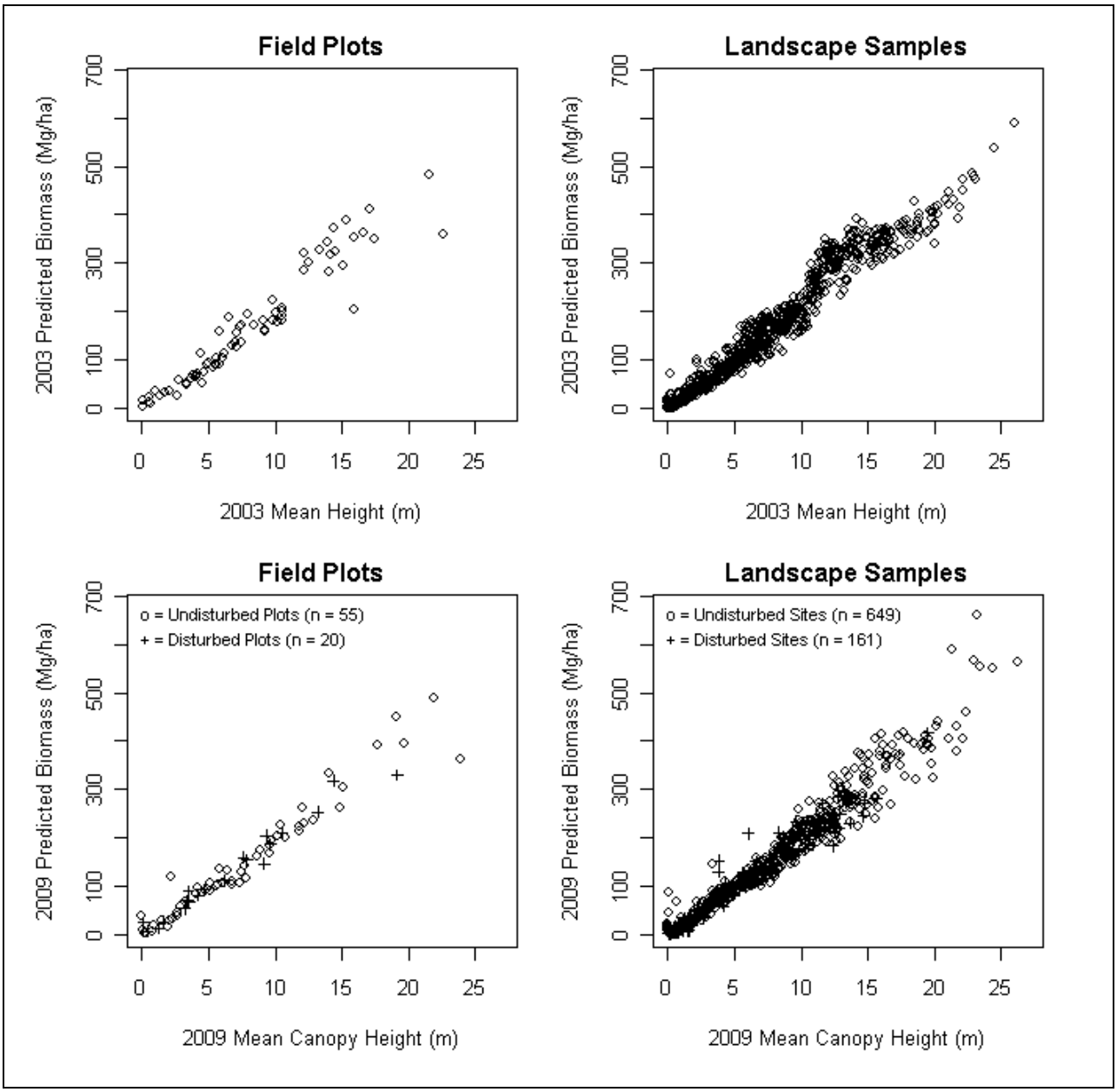

Figure 13: Relationship of predicted aboveground tree biomass to mean canopy height in 2003 (top) and 2009 (bottom) at the field plots (left) and a systematic sample of sites across the landscape (right)

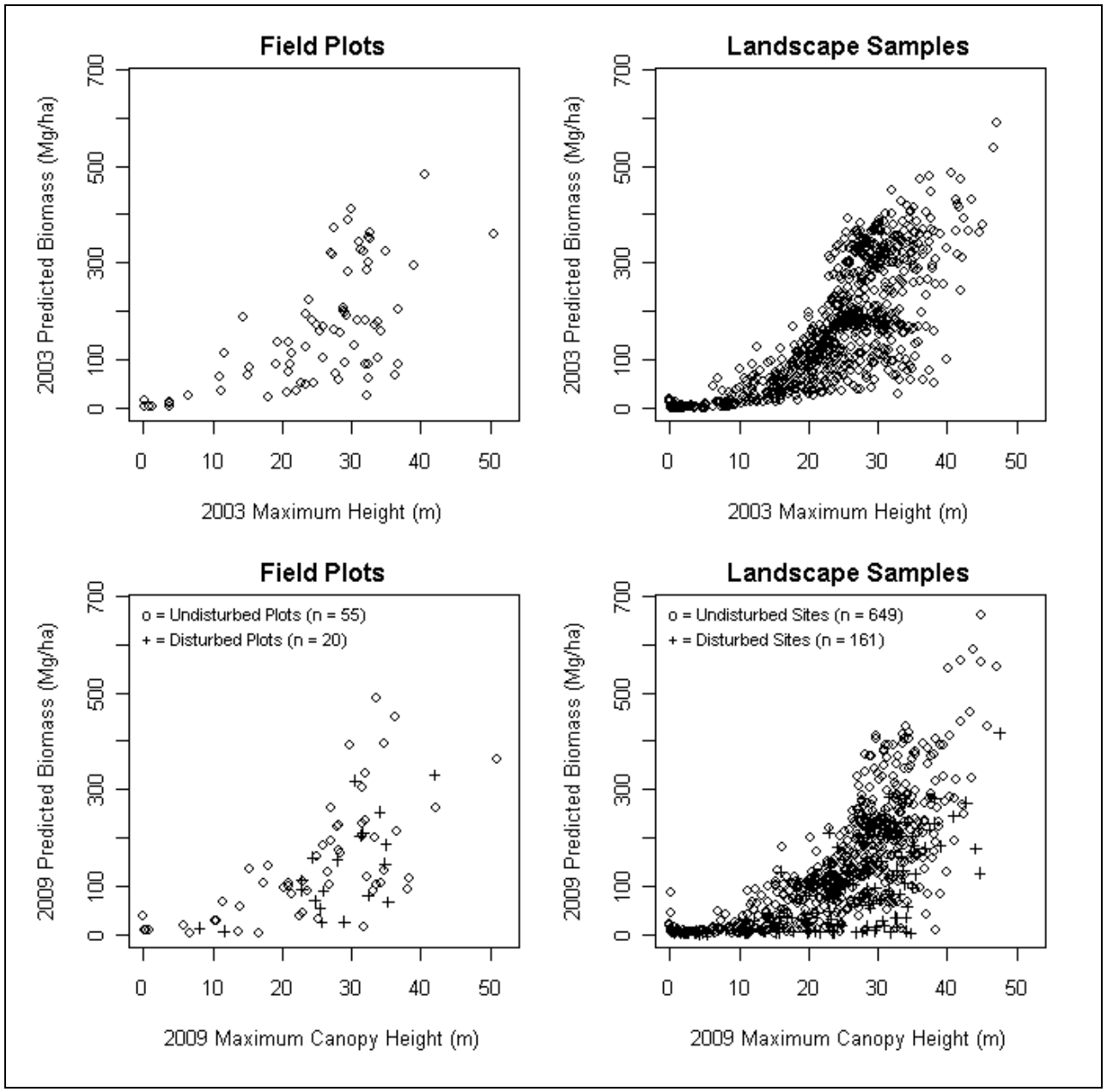

Figure 14: Relationship of predicted aboveground tree biomass to maximum canopy height in 2003 (top) and 2009 (bottom) at the field plots (left) and a systematic sample of sites across the landscape (right).

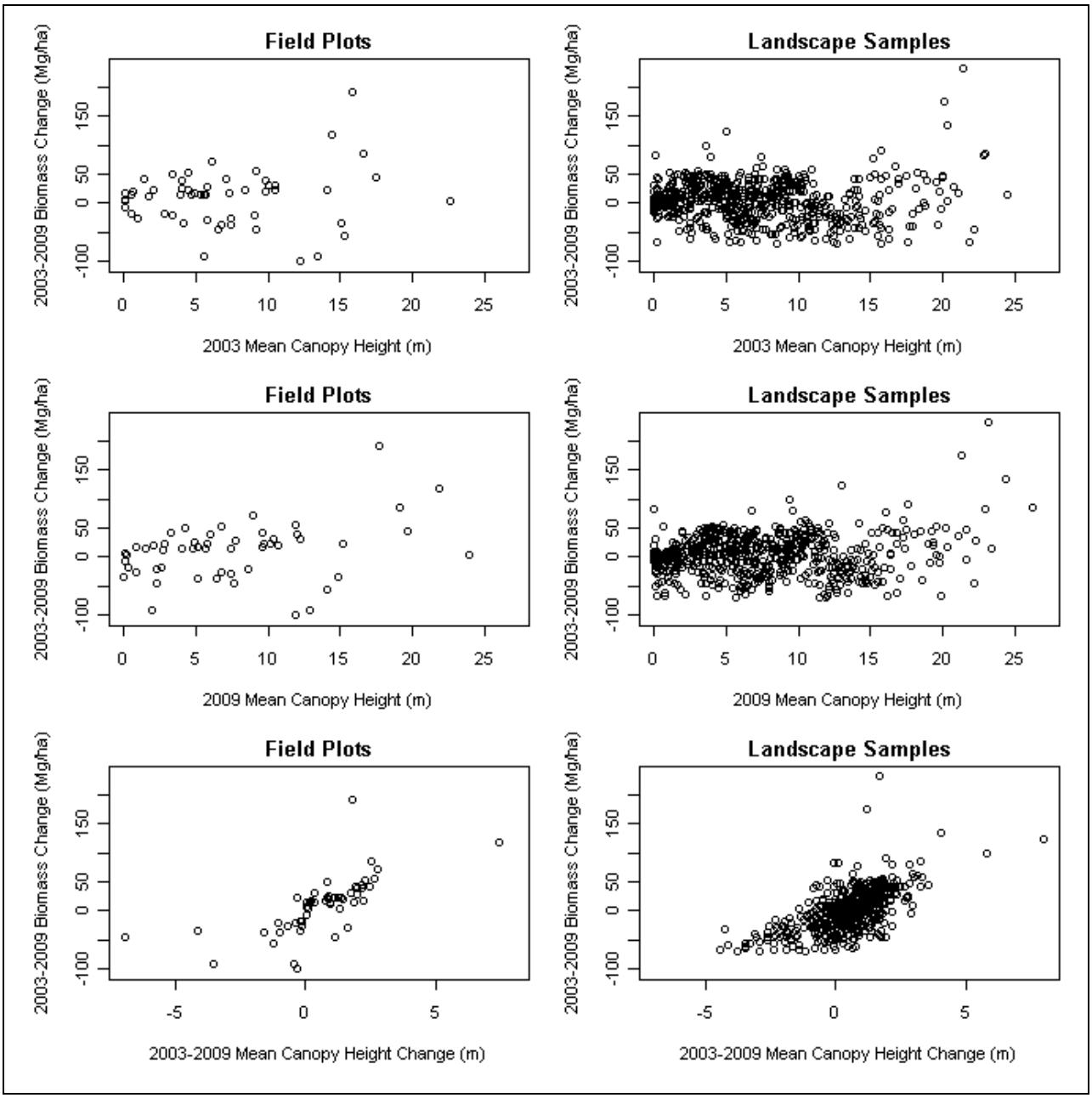

Figure 15: Relationship of biomass change to mean canopy height in 2003 (top), 2009 (middle), and 2003-2009 mean canopy height growth at the undisturbed field plots (left) and systematic sample of undisturbed sites across the landscape (right)

3.2 *Biomass by Successional Stage*

Analysis of variance confirmed that there is an overall difference ($df = 5$, $F = 261$, $p < 0.0001$) in biomass increase within the six successional stages evaluated in this study (Figure 16). We found that the longer the time since disturbance, the greater the accumulation of biomass over the 6-year study period. Biomass accumulation among successional classes was significantly

different, with the exceptions of differences between Stand Initiation (SI) and Understory Reinitiation (UR), and between Young Multistory (YMS) and Mature Multistory (MMS) not being significant ($p > 0.05$).

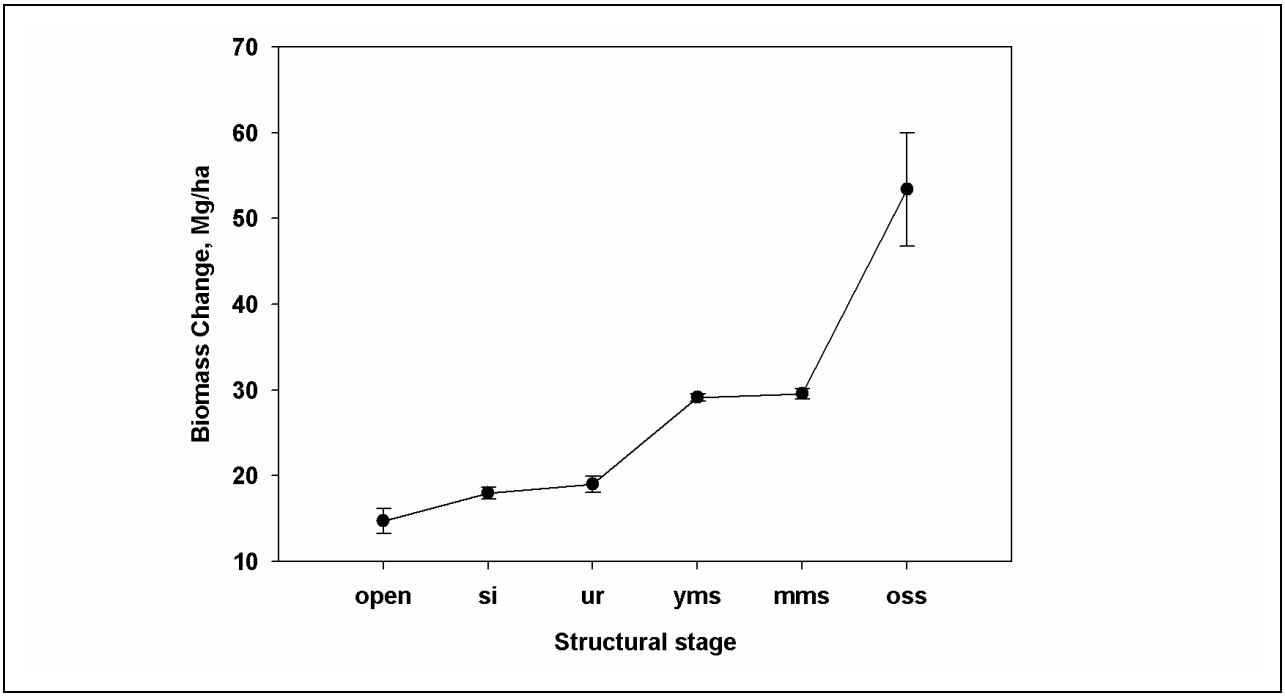

Figure 16: Above ground woody biomass change within previously mapped successional stages. The error bars indicate the 95% confidence intervals. Overall, the biomass change within successional stages is significantly different ($p< 0.0001$). The difference between SI and UR is not significant ($p > 0.05$) and neither is the difference between YMS and MMS; all other pairwise comparisons are significantly different, however.

4. Discussion

4.1 *Effects of Differences in LIDAR Acquisitions*

Both the 2003 and 2009 LiDAR survey landscapes were independently sampled using stratified random sampling designs for distributing field plots in a representative yet unbiased manner. Therefore, our strategy was to treat them as independent assessments. This strategy should prove heartening for others attempting to conduct a biomass/carbon change assessment via repeat LiDAR surveys but with several important considerations.

First, LiDAR sensor capabilities are advancing at a high rate. The 30-fold mean difference in point densities between the 2003 and 2009 LiDAR surveys did not affect our biomass estimates at the plot level, because the distribution of canopy heights was stable (Figure 3). This suggests that if the pulse energy, footprint size, and scan angle are held constant, the probability that a LiDAR pulse will penetrate the canopy, reflect off the ground, and then pass back through the canopy to the sensor should be the same regardless of the pulse density (Table 1). Therefore, LiDAR data from different LiDAR systems (in our case, the ALS40 and ALS50 in 2003 and 2009, respectively) are directly comparable when aggregated to an appropriate scale. The 0.4 points/m^2 mean point density of the 2003 survey translates to a mean of 160 points per 0.25-ha (400 m^2) plot, which is a sufficient number of points to produce a stable canopy height distribution from which to extract canopy height metrics. The mean of 4790 points/plot collected in 2009 represents over-sampling at the plot level of aggregation, but may be sufficiently dense for individual tree characterization in the future, as LiDAR sensor capabilities continue to improve.

Other metrics exhibited the same trends as mean canopy height with regard to the undisturbed vs. disturbed plots (Figure 8), but are not shown for brevity. Maximum canopy height may be a less reliable predictor to compare in our case, because the much higher LiDAR pulse density in 2009 than in 2003 would translate into less height underestimation bias (i.e., higher accuracy) while mean canopy height would not be subject to such a bias.

The selection of locations for field plots based on a landscape stratification will change if the landscape changes, which is a given, or if the extent of the study landscape changes, as was also the case in our study. It is important that the calibration/validation plots represent the landscape in a representative yet unbiased manner. This can be accomplished through random or random stratified sampling designs conditioned on the spatial extent of the landscape they represent, or systematic monitoring plots as used by the USFS Forest Inventory and Analysis program (FIA). The coarse spatial frequency of FIA plots relative to this and most other LiDAR project areas requires more intensive localized sampling to adequately characterize the range of variability in forest structure conditions of interest.

4.2 *Biomass Gains by Successional Stage*

Assessing biomass accumulation over large areas and extended time periods is essential for improved estimates of carbon pools and fluxes and potential effects on the global carbon budget (Strand et al. 2008). Stand age has been shown by several researchers to affect ecosystem carbon uptakes. For example, Law et al. (2003) recorded differences in carbon accumulation rates along a chronosequence after a clearcut in ponderosa pine (*Pinus ponderosa*) in Oregon. Young

regenerating stands were found to lose carbon to the atmosphere, while older stands were accumulating carbon up to an age of 100-200 years of age when the carbon accumulation rates were reduced again. Similarly, Schwalm et al. (2007) recorded carbon loss in young stands (< 20 years) followed by an increased ecosystem net primary productivity with increased stand age in Douglas-fir (*Pseudotsuga meziesii*) in British Columbia using eddy covariance flux measurements. Although successional stages are not necessarily related to stand age, we found that successional stages containing mature and old trees stored more carbon over a six year time period than did stands composed of younger trees (Figure 8). Because the majority of the study area is managed, and harvest has occurred in most places within the past 100 years, we did not expect to find a decrease in biomass accumulation for successional stages dominated by large trees at this point in time. Potentially, a future lack of disturbance in the area would lead to decreased carbon accumulation at some point in time; however, the current data did not allow us to test this hypothesis.

4.3 ***Sources of Error***

Although 75 of the 2003 field plots were re-measured in 2009, they were unfortunately not marked with permanent monuments in 2003, only geolocated with differential GPS to a horizontal uncertainty of <2m. The 2009 field crews placed (and geolocated also with differential GPS) the 2009 plot centers as nearly as possible to the 2003 plot center locations, but the differences between 2003 and 2009 plot locations vary from 0.46 m to 9.25 m with a mean of 2.67 m and a standard deviation of 1.65 m. These mismatches do not include the additive uncertainties in the 2003 and 2009 plot locations. This geolocation error can amount to a large source of error at the fine scale of canopy structure variation that is undoubtedly contributing greatly to the scatter in the biomass change estimates illustrated in Figs. 6-7. The results are nevertheless encouraging because these errors should be randomly distributed, which is why the mean estimates of predicted biomass change in Fig. 7 are reasonable. This is the major reason we have presented only independent 2003 and 2009 biomass models in this report, rather than an attempt to model biomass change directly.

Our solution for model refinement is to reconcile the 2003 and 2009 tree lists, since trees have the useful quality of immobility. The trees also were not labeled by permanent tree tags in 2003, only temporary ones. However, the distance and bearing to measured trees was recorded. Therefore, by graphically comparing the plot-level stem maps and identifying the same trees, we can calculate x and y offsets between the 2003 and 2009 plot locations and adjust them accordingly. Recalculating plot-level LiDAR metrics from the corrected plot footprints should lead to more consistent predictions and greatly reduce the scatter in Figs. 5-7, particularly the undisturbed plots in Figs. 6-7 that would exhibit greater sensitivity to shifted plot footprints.

5. Conclusion

In this study, we demonstrate the utility of using multi-temporal discrete return airborne LiDAR surveys in concert with field sampling and statistical modeling techniques to quantify spatiotemporal patterns of aboveground biomass accumulation in a heavily managed conifer forest. This forest is representative of many forests around the globe in that it is managed by multiple user groups, including industrial forestry companies, private owners, and public land managers. The results of this study indicate that multi-temporal LiDAR is an accurate method that is viable for monitoring broad-scale changes in aboveground forest biomass across large tracts of land. As LiDAR data become continually more available across a range of biomes, we expect that this approach will assist with quantifying the amount of carbon stored in forest ecosystems and therefore support current and future efforts to mitigate increasing levels of atmospheric CO_2.

6. References

Coops, N. C., Waring, R. H., and Landsberg, J. J. 1998. Assessing forest productivity in Australia and New Zealand using a physiologically-based model driven with averaged monthly weather data and satellite derived estimates of canopy photosynthetic capacity. Forest Ecology and Management 104: 113-127.

Evans, J.S. and S.A. Cushman. 2009. Gradient Modeling of Conifer Species Using Random Forest. Landscape Ecology 5:673-683.

Evans J.S., M.A. Murphy, Z.A. Holden, S.A. Cushman. 2010. Modeling species distribution and change using Random Forests. Chapter 8 in Predictive Modeling in Landscape Ecology eds Drew, CA, Huettmann F, WiersmaY. Springer.

FRA (2005). Global Forest Resource Assessment 2005. Progress towards sustainable forest management. Food and Agriculture Organization of the United Nations Forestry Paper 147, Viale delle Terme di Caracalla, Rome, Italy. Internet access: http://www.fao.org/docrep/008/a0400e/a0400e00.htm

Fu, P. and P.M. Rich, 1999. Design and implementation of the Solar Analyst: an ArcView extension for modeling solar radiation at landscape scales. Proceedings of the 19th Annual ESRI User Conference, San Diego, USA. http://www.fs.fed.us/informs/download.php

Gonzalez, P., G.P. Asner, J.J Battles, M.A.. Lefsky, K.M. Waring, and M. Palace. 2010. Forest carbon densities and uncertainties from LiDAR, QuickBird, and field measurements in California, Remote Sensing of Environment 114: 1561-1575

Harmon, M.E. and B. Marks. 2002. Effects of silvacultural practices on carbon stores in Douglas-fir – western hemlock forests in the Pacific Northwest, U.S.A.: Results from a simulation model. *Canadian Journal of Forest Research* 32: 863-877.

Hollinger D.Y.and A. D. Richardson, 2005. Uncertainty in eddy covariance measurements and its application to physiological models. Tree Physiology 25: 873– 885.

Hudak, A.T., M.A. Lefsky, W.B. Cohen and M. Berterretche. (2002) Integration of LiDAR and Landsat ETM+ data for estimating and mapping forest canopy height. *Remote Sensing of Environment* 82(2-3): 397-416.

Hudak A.T., N.L. Crookston, J.S. Evans, D.E. Hall, M.J. Falkowski. 2008. Nearest neighbor imputation of species-level, plot-scale forest structure attributes from LiDAR data. Remote Sensing of Environment 112: 2232–2245.

Landsberg, J. J. and Waring, R. H. 1997. A generalized model of forest productivity using simplified concepts of radiation use efficiency, carbon balance and partitioning. Forest Ecology and Management 95: 209-228.

Law, B.E., P.E. Thornton, J. Irvine, P.M. Anthoni, and S. VanTuyl (2001), Carbon storage and fluxes in ponderosa pine forests at different developmental stages, *Global Change Biology, 7*, 755-777.

Law, B.E., O.J. Sun, J. Campbell, S. Van Tuyl, and P.E. Thornton (2003), Changes in carbon storage and fluxes in a chronosequence of ponderosa pine, *Global Change Biology, 9*, 510-524.

Lefsky, M.A., W.B. Cohen, S.A. Acker, G.G. Parker, T.A. Spies, and D. Harding. 1999. LiDAR remote sensing of the canopy structure and biophysical properties of Douglas-fir werstern hemlock forests. Remote Sensing of Environment 70: 339-361.

Lefsky, M.A., W.B. Cohen, D.J. Harding, G.G. Parker, S.A. Acker, and S.T. Gower. 2002. LiDAR remote sensing of aboveground biomass in three biomes. *Global Ecology and Biogeography* 11: 393-399.

Martinuzzi, S., Vierling, L.A., Gould, W.A., Falkowski, M., Evans, J.S., Hudak, A.T., and Vierling, K.T. (2009). Mapping snags and understory shrubs for a LiDAR-based assessment of wildlife habitat suitability. *Remote Sensing of Environment*, 113: 2533–2546.

Murphy M.A., J.S. Evans, and A.S. Storfer (2010) Quantify Bufo boreas connectivity in Yellowstone National Park with landscape genetics. Ecology 91:252-261

Nilsson, M. 1996. Estimation of tree heights and stand volume using an airborne LiDAR system. Remote Sensing of Environment 56: 1-7

R Development Core Team (2007). R: A language and environment for statistical computing. Vienna, Austria: R Foundation for Statistical Computing. Access: http://www.R-project.org.

Running, S.W. and J.C. Coughlan (1988) A general model of forest ecosystem processes for regional applications, I. Hydrologic balance, canopy gas exchange and primary production processes. Ecol.Model., 42, 125-154.

Running, S.W. and S.T. Gower (1991) FOREST-BGC, a general model of forest ecosystem processes for regional applications, II. Dynamic carbon allocation and nitrogen budgets. Tree Physiol., 9, 147-160.

Schwalm C.R, T.A. Black, K. Morgenstern and E.R. Humphreys, 2007. A method for deriving net primary productivity and component respiratory fluxes from tower-based eddy covariance data: a case study using a 17-year data record from a Douglas-fir chronosequence. Global Change Biology 13:370–385.

Strand E.K., L.A. Vierling, A.M.S. Smith, S.C. Bunting. 2008. Net changes in aboveground woody carbon stock in western juniper woodlands, 1946–1998. Journal of Geophysical Research 113: G01013, doi:10.1029/2007JG000544.

Vine, E., and J. Sathaye. 1997. The monitoring, evaluation, reporting, and verification of climate change mitigation projects: Discussion pf issues and methodologies and review of existing protocols and guidelines, EPA Report LBNL-40316

Waring, R.H., N.C. Coops, J.J. Landsberg. 2010. Improving predictions of forest growth using the 3-PGS model with observations made by remote sensing, Forest Ecology and Management 259: 1722-1729

Appendix A: Presentations and manuscripts associated with this project

Presentations

Hudak, A., E. Strand and L. Vierling. Utility of remotely sensed data for future forest inventory and monitoring. International Forestry Student Association (IFSA) Symposium, Kookmin University, Seoul, South Korea, 20 Aug 2010 (invited).

Hudak, A., E. Strand and L. Vierling. Assessment of coniferous forest carbon sequestration in the Northern Rockies, USA using LiDAR remote sensing, field surveys, and a forest growth model. International Union of Forestry Research Organizations (IUFRO) World Congress, Seoul, South Korea, 24 Aug 2010.

Vierling, L.A., Martinuzzi, S., Hudak, A.T., Garrity, S.R., Eitel, J.U.H., Strand, E.K., Falkowski, M.J., and Vierling, K.T. Landsat Time Series-based Vegetation Change: Context for Understanding Ecological Legacies. Landsat Science Team Semi-Annual Meeting, Boise, ID, 16 June 2010 (invited).

Vierling, L.A., Strand, E.K., Eitel, J.U.H., and Hudak, A.T. 200 kilohertz and a Cessna: Using lasers to measure forest dynamics for global carbon accounting. University of Idaho, April, 2010.

Hudak, A.T., Strand, E.K., and Vierling, L.A. Quantifying growth and disturbance effects on forest biomass from repeated field plot and LiDAR measures. USFS Rocky Mountain Research Station All-Scientists Meeting, Fort Collins, CO, March, 2010.

Hudak, A., L. Vierling and E. Strand. Using multi-temporal LiDAR to quantify biomass change. Inland Northwest Growth & Yield (INGY) Cooperative Annual Winter Technical Meeting, Spokane, Washington, 9 Mar 2010.

Vierling, L.A., Hudak, A.T., and Strand, E.K. "Big Sky C Sequestration Partnership Forest Aboveground Carbon Assessment: Preliminary Validation". Big Sky Carbon Sequestration Partnership Annual Meeting, Bozeman, MT, September, 2009.

Manuscripts in preparation

Strand, E. K., Hudak, A.T., Vierling, L.A., Martinuzzi, S., and Eitel, J.U.H. Quantifying Forest Aboveground Carbon Pools and Fluxes Using Multi-temporal LiDAR. JGR-Biogeosciences, in preparation.

Hudak, A.T., Eitel, J.U.H., Vierling, L.A., Strand, E.K., and Martinuzzi, S. Using LiDAR and species-specific growth information to model aboveground carbon storage in the Inland Northwest. Ecological Modelling, in preparation.

Vierling, L.A., Eitel, J.U.H., Martinuzzi, S., Hudak, A.T., and Strand, E.K. Terrestrial and airborne laser scanner data for assessing tree height: implications for biomass estimation in conifer forests. Remote Sensing of Environment, in preparation.

Eitel, J.U.H., Vierling, L.A., Hudak, A.T., Strand, E.K., and Martinuzzi, S. The use of red-edge spectral data from the RapidEye satellite to predict and improve estimates of aboveground carbon storage in a conifer forest. Remote Sensing of Environment, in preparation.